Hydrogen therapy after resuscitation improves myocardial injury involving inhibition of autophagy in an asphyxial rat model of cardiac arrest

XIAOHUI GONG[1-7*], XINHUI FAN[1,3-6*], XINXIN YIN[1,3-6], TONGHUI XU[1,3-6], JIAXIN LI[1,3-6], JIALIN GUO[1,3-6], XIANGKAI ZHAO[1,3-6], SHUJIAN WEI[1,3-6], QIUHUAN YUAN[1,3-6], JIALI WANG[1,3-6], XUCHEN HAN[2,7] and YUGUO CHEN[1,3-6]

[1]Department of Emergency Medicine, Qilu Hospital of Shandong University, Cheeloo College of Medicine, Shandong University, Jinan, Shandong 250012; [2]Department of Emergency Medicine, Affiliated Hospital of Chifeng University, Chifeng, Inner Mongolia Autonomous Region 024005; [3]Shandong Provincial Clinical Research Center for Emergency and Critical Care Medicine, Institute of Emergency and Critical Care Medicine of Shandong University, Chest Pain Center, Qilu Hospital of Shandong University; [4]Key Laboratory of Emergency and Critical Care Medicine of Shandong Province, Key Laboratory of Cardiopulmonary-Cerebral Resuscitation Research of Shandong Province; [5]Shandong Provincial Engineering Laboratory for Emergency and Critical Care Medicine, Qilu Hospital of Shandong University; [6]Key Laboratory of Cardiovascular Remodeling and Function Research, Chinese Ministry of Education, Chinese Ministry of Health and Chinese Academy of Medical Sciences, The State and Shandong Province Joint Key Laboratory of Translational Cardiovascular Medicine, Qilu Hospital of Shandong University, Jinan, Shandong 250012; [7]Institute of Cardiovascular Disease of Chifeng University, Chifeng, Inner Mongolia Autonomous Region 024005, P.R. China

Received November 20, 2021; Accepted March 21, 2022

DOI: 10.3892/etm.2022.11302

Abstract. Hydrogen (H_2) therapy is a therapeutic strategy using molecular H_2. Due to its ability to regulate cell homeostasis, H_2 therapy has exhibited marked therapeutic effects on a number of oxidative stress-associated diseases. The present study investigated the effectiveness of H_2 therapy in protecting against myocardial injury in a rat model of asphyxial cardiac arrest and cardiopulmonary resuscitation. Rats underwent 10-min asphyxia-induced cardiac arrest (CA) and cardiopulmonary resuscitation (CPR), and were randomly divided into control and H_2 therapy groups. After resuscitation, the H_2 therapy group was administered room air mixed with 2% H_2 gas for respiration. During CA/CPR, the arterial pressure and heart rate were measured every minute. Survival rate, cardiac function, myocardial injury biomarkers creatine kinase-MB and cardiac troponin-T, and histopathological changes were evaluated to determine the protective effects of H_2 therapy in CA/CPR. Immunohistochemistry and western blot analysis were used to determine the expression levels of autophagy-associated proteins. *In vitro*, H9C2 cells were subjected to hypoxia/reoxygenation and H_2-rich medium was used in H_2 treatment groups. Western blotting and immunofluorescence were used to observe the expression levels of autophagy-associated proteins. Moreover, an adenovirus-monomeric red fluorescent protein-green fluorescent protein-LC3 construct was used to explore the dynamics of autophagy in the H9C2 cells. The results showed that H_2 therapy significantly improved post-resuscitation survival and cardiac function. H_2 therapy also improved mitochondrial mass and decreased autophagosome numbers in cardiomyocytes after resuscitation. The treatment inhibited autophagy activation, with lower expression levels of autophagy-associated proteins and decreased autophagosome formation *in vivo* and *vitro*. In conclusion, H_2 gas inhalation after return of spontaneous circulation improved cardiac function via the inhibition of autophagy.

Correspondence to: Dr Yuguo Chen, Shandong Provincial Clinical Research Center for Emergency and Critical Care Medicine, Institute of Emergency and Critical Care Medicine of Shandong University, Chest Pain Center, Qilu Hospital of Shandong University, 107 Wen Hua Xi Road, Jinan, Shandong 250012, P.R. China
E-mail: chen919085@sdu.edu.cn

Dr Xuchen Han, Department of Emergency Medicine, Affiliated Hospital of Chifeng University, 42 Wangfu Street, Songshan Area, Chifeng, Inner Mongolia Autonomous Region 024005, P.R. China
E-mail: hanxuchen2004@163.com

*Contributed equally

Key words: hydrogen therapy, cardiac arrest, cardiopulmonary resuscitation, myocardial injury, autophagy, beclin-1

Introduction

Cardiac arrest (CA) is a global public health concern with a low resuscitation rate and a high mortality rate (1,2). Despite improvements in cardiopulmonary resuscitation (CPR) and post-resuscitation care in recent years, the post-discharge survival rate of patients with return of spontaneous circulation (ROSC) is less than one-third of all cases (3-6). Myocardial dysfunction along with the systemic ischemia/reperfusion (I/R) injury that occurs during CPR is a primary cause for the poor prognosis of patients after ROSC (7). Thus, protection of myocardial function after CA is essential and of significant value.

Although the mechanism of CPR-induced myocardial injury is not fully understood, systemic I/R-induced reactive oxygen species (ROS) has been widely demonstrated as a critical factor (8-10). CA/ROSC is a global I/R event accompanied by ROS generation. Moreover, the accumulation of ROS is further exacerbated after ROSC owing to oxygenated blood returning to the tissues, which generates oxidation of cell macromolecular substances (9,11). Generally, oxidative stress events, featuring excessive production of ROS, have been recognized as serving a key role in cell damage, mitochondrial dysfunction, and ultimately cell apoptosis and death (12).

Restoring spontaneous circulation and preventing hypoxic ischemic tissue injury are the goals of CPR (13). As sufficient oxygen delivery is required to restore and maintain the energy state of the heart, the use of maximal inspired oxygen (O_2) concentrations during CPR and of earlier post-resuscitation are recommended in the European Resuscitation Council Guidelines 2021 (14). However, a considerable amount of data has emerged challenging the appropriateness of the use of 100% O_2 during and after resuscitation from CA (15,16). Hyperoxia has been shown to increase the generation of ROS, resulting in aggravated reperfusion myocardial injury and worsened CPR outcomes (17).

Hydrogen (H_2) gas is a type of endogenous gas transmitter produced by the intestinal flora during the fermentation of nondigestible carbohydrates (18). Previous, studies have demonstrated that molecular H_2 is a new type of safe and effective therapeutic agent (19,20). In addition, studies to date have found that H_2 therapy significantly protects against oxidative stress and inflammation-related diseases, such as cancer, atherosclerosis, diabetes, I/R injury, neurodegenerative diseases, arthritis, hepatitis and pancreatitis (21-24). Based on its safety and wide effectiveness, H_2 therapy is attracting increasing attention and is undergoing an important evolution from bench to bedside (19,25). In previous studies, H_2 inhalation without hyperoxia after resuscitation improved the neurological outcome in rat models of CA (26,27). However, the effects of H_2 inhalation on CA/CPR-induced myocardial injury remain poorly understood. Therefore, the present study used H_2 inhalation in post-resuscitation care to investigate its effect on myocardial injury induced by CA in rats.

Materials and methods

Animals. A total of 60 adult male Wistar rats (age, 10-12 weeks; weight, 400-450 g) were purchased from the Experimental Animal Center of Shandong University (Jinan, China). All animals were housed together in a room maintained at 40-60% relative humidity and 23±2˚C, with 12-h light/dark cycles and *ad libitum* access to food and water. All animal experiments were approved by the Animal Care and Use Committee of the Qilu Hospital of Shandong University (Jinan, China; approval no. KYLL-2020-ZM-122), and adhered to the Care and Use of Laboratory Animals guidelines and to the Animal Research: Reporting of *In Vivo* Experiments guidelines. All animal experiments took place at Shandong Provincial Engineering Laboratory for Emergency and Critical Care Medicine, Qilu Hospital of Shandong University. All animals were anesthetized with phenobarbital sodium and then sacrificed with carbon dioxide release devices.

Rat model of asphyxial CA. The 10-min asphyxial CA/CPR model was used in this study. Rats were randomly assigned to the following four groups (n=15 per group): i) Sham + normoxia (anesthetized with 4% isoflurane mixed with room air and normoxia inhalation by ventilator for 2 h); ii) Sham + H_2 (anesthetized with 4% isoflurane mixed with room air and H_2 inhalation by ventilator for 2 h); iii) CPR + normoxia (anesthetized with 4% isoflurane mixed with room air, CA/CPR treatment and normoxia inhalation by ventilator for 2 h after ROSC); and iv) CPR + H_2 (anesthetized with 4% isoflurane mixed with room air, CA/CPR treatment and H_2 inhalation using a ventilator for 2 h after ROSC). Rats were anesthetized with 4% isoflurane mixed with room air and were under tracheal intubation with connection to a ventilator. Intravascular catheters were placed into the right femoral artery and right vein for blood pressure monitoring and drug administration, respectively. After stabilization for 20 min, the ventilator was disconnected to induce CA. Circulatory arrest was determined by cessation of the arterial pulse and a mean arterial pressure (MAP) of <20 mmHg. After 10 min of asphyxia, CPR was performed, with inhalation of air with a ventilator and intravenous administration of epinephrine (0.01 mg/kg). In addition, the rate of artificial chest compressions was ~200 per min. Epinephrine (0.02 mg/kg) was administered at 2-min intervals until ROSC was achieved. ROSC was defined by an MAP of >60 mmHg that lasted for at least 10 min. A total of 3 rats with ROSC failure within 5 min or those that could not be disengaged from the ventilator after observation for 1 h were excluded from the study. The core temperature of each rat was maintained at 37.0±0.5˚C. After ROSC, gas inhalation was continued for 2 h (Fig. 1A): Premixed gas (1.3% H_2 and 26% O_2) was used in the H_2 therapy groups, and normoxia (26% O_2) was used as the control (27). Following this, the rats were euthanized by exposure to a gradually increasing concentration of CO_2 (the flow rate was 50% of the chamber volume/min).

Cell culture. H9C2 cells were purchased from the American Type Culture Collection and cultured in Dulbecco's modified Eagle's medium (Gibco; Thermo Fisher Scientific, Inc.) supplemented with 10% FBS (Gibco; Thermo Fisher Scientific, Inc.) and 100 U/ml penicillin + 100 mg/ml streptomycin in a cell incubator (95% air and 5% CO_2) at 37˚C. In the cell hypoxia/reoxygenation (H/R) model, H9C2 cells were exposed to hypoxia (5% CO_2 and 1% O_2 at 37˚C) for 24 h and reoxygenation (95% air and 5% CO_2) for 4 or 12 h.

H_2 treatment in vitro. In the H_2 treatment group, H_2-rich medium was used to culture the H92C cells instead of normal

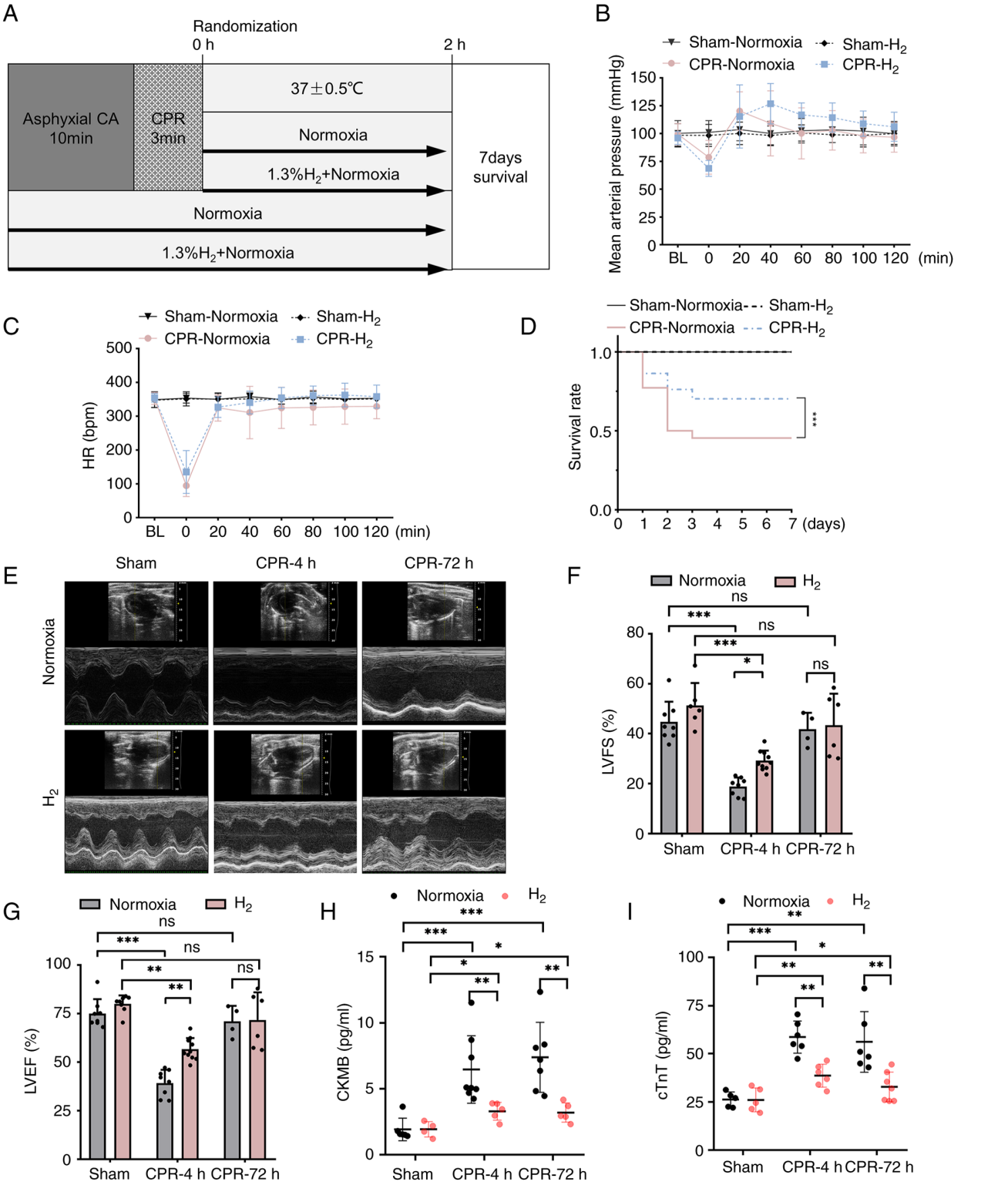

Figure 1. Inhalation of H_2 gas after ROSC improves post-resuscitation survival and cardiac function. (A) The experimental process for CPR and post-resuscitation care in the rat model of asphyxial CA/CPR. (B and C) The MAP and heart rate of rats during asphyxial CA/CPR. (D) The survival rate of rats in each group were recorded for 7 days after asphyxial CA/CPR (n=10). (E-G) Representative images and quantitative assessment of LVFS and LVEF evaluated by echocardiography (n=8-10). (H and I) The serum levels of CKMB and cTnT (n=5). *P<0.05, **P<0.01 and ***P<0.001. ROSC, return of spontaneous circulation; MAP, mean arterial pressure; H_2, hydrogen molecule; HR, heart rate; CA, cardiac arrest; CPR, cardiopulmonary resuscitation; LVFS, left ventricular fraction shortening; LVEF, left ventricular ejection fraction; CKMB, creatine kinase-MB; cTnT, cardiac troponin T.

DMEM. H_2 was diluted into cell culture medium to produce an H_2-rich culture medium (0.6 mmol/l) (28). The H_2-rich medium was freshly prepared for each experiment. DMEM was used as the vehicle.

Transmission electron microscopy (TEM). Part of the left ventricle (LV) was obtained from the rats and fixed quickly in 2% glutaraldehyde and 2% paraformaldehyde in 0.1 M phosphate buffer (pH 7.4) at room temperature for 2 h. After

3 washes in phosphate-buffered saline, tissues were fixed and stained using 1% osmium tetroxide on 4˚C for 2 h and washed 3 times in phosphate-buffered saline. After ethanol dehydration, samples were embed in LX112 resin (Ladd Research Industries) at room temperature for 2 h. Ultrathin sections (~70 nm) were obtained with a MT-X ultramicrotome (Leica EM UC7; Leica Microsystems, Inc.) and observed using an electron microscope (H-7650; Hitachi, Ltd.). Images of sections were assessed using ImageJ (V1.8.0.112; National Institutes of Health).

Mitochondrial mass quantification. The TEM images were processed using ImageJ V1.8.0.112. The outline of each mitochondrion was precisely drawn using a Surface Pro 6 tablet equipped with a touch pen (Microsoft Corporation), and filled with a solid bright color. The image with color-filled mitochondria was converted into a binary black and white image using the 'color threshold' command, and areas of mitochondria were then generated using the 'analyze particles' command. Briefly, this command recognized the black objects (mitochondria) in the binary images and outlined them such that the area of each outlined object was automatically computed. Fractional area was calculated as total mitochondrial area divided by image area for the cardiomyocytes. Mitochondrial number and average mitochondrial area (an indication of mitochondrial size) were also measured (29).

Western blotting. Samples (left ventricle tissues from rats and H9C2 cells) were lysed with RIPA buffer (Beyotime Institute of Biotechnology) for 30 min on ice. After centrifugation at 12,000 rpm for 10 min at 4˚C, the supernatant was transferred to a new tube. PMSF (1:100) was added, and a BCA kit (Beyotime Institute of Biotechnology) was used to determine protein concentration. Proteins (20 μg) were separated using 10% SDS-PAGE and transferred onto PVDF membranes. After blocking with 5% milk in PBS at room temperature for 2 h, the membranes were incubated with primary antibodies at 4˚C overnight. The membranes were washed three times with TBS-Tween-20 (TBS-T) and incubated with secondary antibody (dissolved in 1% BSA; 1:5,000) at room temperature for 1 h. After being washed with TBS-T three times, the membranes were exposed to ECL substrate (Beyotime Institute of Biotechnology; catalog no. P0018FS) and detected by the chemiluminescence method in an AI600 gel imaging system (GE Healthcare). The following primary antibodies were used: Anti-Beclin-1 (catalog no. ab223348; 1:1,000), anti-LC3B (catalog no. ab51520; 1:1,000), anti-p62 (catalog no. ab109012; 1:1,000) and anti-β-actin (catalog no. ab8226; 1:1,000) (all Abcam). The secondary antibodies were goat anti-rabbit IgG H&L (HRP) (catalog no. ab205718; 1:5,000) and goat anti-mouse IgG H&L (HRP) (catalog no. ab6789; 1:5,000) (both Abcam).

Immunohistochemical analysis. Rats tissues were fixed with 4% polyformaldehyde at room temperature for 24 h, then dehydrated with alcohol and washed with xylene. The tissues were embedded in a wax block and sliced to a 5-μm thickness. Dewaxing agent was used to dewax the sections at 55˚C for 1 h, and different concentrations of alcohol (100, 95, 90, 80, 70, 60 and 50%, for 30 min each) were used to wash the sections. According to the instructions of the SABC-POD kit (Boster Biological Technology; catalog no. SA1028), sections were incubated with 3% H_2O_2 at room temperature for 5 min, and infiltrated into 0.01 M Citrate Antigen Retrieval solution (Wuhan Servicebio Technology Co., Ltd.; catalog no. G1201-1L) at 100˚C for 20 min. To cool them down to room temperature, sections were washed three times with PBS (phosphate-buffered saline). After blocking with 5% BSA (Wuhan Servicebio Technology Co., Ltd.; catalog no. SW3015) at 37˚C for 30 min, sections were incubated with primary antibodies at 4˚C overnight. Next, the sections were washed three times with PBS, and incubated with anti-rabbit IgG H&L (HRP; 1:1,000; cat. no. ab205718; Abcam) and goat anti-mouse IgG H&L (HRP; 1:1,000; cat. no. ab6789; Abcam) at 37˚C for 30 min. After washing three times with PBS, the sections were incubated with SABC at room temperature for 20 min. Finally, sections were incubated with DAB substrate (Boster Biological Technology; catalog no. AR1022) and washed with ddH_2O. Sections were redyed with hematoxylin for 30 sec, dehydrated with inversed different concentrations of alcohol and sealed with Permount™ Mounting Medium (Sangon Biotech, Co., Ltd.; catalog no. E675007). Immunohistochemical staining was performed with anti-LC3B (1:1,000). Images of sections were captured (IX53; Olympus Corporation) and assessed (ImageJ V1.8.0.112) according to the percentage of stained cells (total original magnification, x40; area, 250x250 μm).

Immunofluorescence analysis and confocal microscopy. H9C2 cells were incubated with the aforementioned primary antibodies to evaluate the levels of Beclin-1 (1:100) and LC3B (1:100). Samples were incubated with DAPI after washing three times with PBS at room temperature, and then sealed with coverslips immediately. Images of cells were taken using confocal laser scanning fluorescence microscopy (SP8; Leica Microsystems GmbH).

Evaluation of fluorescent LC3 punctae. The changing fluorescent punctae of LC3 in H9C2 cells were observed with a tandem red fluorescent protein (RFP)-green fluorescent protein (GFP)-LC3 construct (Ad-RFP-GFP-LC3). Ad-RFP-GFP-LC3 adenovirus was purchased from ViGene Biosciences (Charles River Laboratories, Inc.). H9C2 cells (American Type Culture Collection; cat. no. CRL-1446) were transfected with Ad-RFP-GFP-LC3 at 50 MOI. In brief, H9C2 cells were inoculated into a 24-well plate at a density of $1x10^5$ cells/well. A total of 250 μl of DMEM containing 1% FBS (both Thermo Fisher Scientific, Inc.), 100 μl adenovirus (10^6 PFU/ml; ViGene Biosciences; Charles River Laboratories, Inc.) and 100 μl Lipofectamine 2000® reagent (Invitrogen; Thermo Fisher Scientific, Inc.) was added to each well. After mixing, the cells were cultured for 6 h in an incubator containing 5% CO_2 at 37˚C. After 6 h, the adenovirus was moved off and the transfected cells were cultured for 48 h continuously. The green and red fluorescence intensities were assessed under laser scanning fluorescence microscopy (SP8; Leica Microsystems GmbH). Images of sections were assessed (ImageJ software V1.8.0.112; National Institutes of Health) according to the numbers of red and yellow dots in each cell (total original magnification, x63).

Ultrasonic cardiogram. Under isoflurane anesthesia, the spontaneous breathing of the rats was maintained. The two-dimensional images of the LV [left ventricular fraction shortening (LVFS) and left ventricular ejection fraction (LVEF)] were collected using ultrasonic cardiogram equipment (Vevo2100; VisualSonics, Inc.) on the short-axis and long-axis section of the parasternal papillary muscles. The two-dimension-guided M-mode or B-mode ultrasonic cardiogram of 10 cardiac cycles was obtained. Images were assessed using Vevo2100 software.

Creatine kinase-MB (CKMB) and cardiac troponin-T (cTnT) measurement. Blood was collected at sacrifice and then the serum was isolated using centrifugation (1,000 g; 4˚C for 15 min). The serum concentrations of CKMB (Cloud-Clone Corp.; catalog no. SEA479Ra) and cTnT (Cloud-Clone Corp.; catalog no. SED232Ra) were measured by ELISA kit following the manufacturer's instructions.

Statistical analysis. The statistical significance was performed using GraphPad Prism 8 (GraphPad Software, Inc.) Differences between groups were estimated using one-way ANOVA followed by Tukey's post hoc test. Comparisons across two variables were used a two-way ANOVA followed by Tukey's post hoc test. $P<0.05$ was considered to indicate a statistically significant difference. All data are expressed as the mean ± standard error.

Results

Inhalation of H_2 gas after ROSC improves post-resuscitation survival and cardiac function. As shown in Fig. 1B and C, there were no statistical differences in MAP and heart rate during post-resuscitation care whether using inhalation of H_2 gas or not. The survival rate of the rats was recorded continuously for 7 days after CA/CPR (Fig. 1D). In the Sham groups, the survival rate was 100% whether using inhalation of H_2 gas or not. However, compared with that in the normoxia groups, the survival rate at 7 days after ROSC was significantly higher following inhalation of H_2 gas during post-resuscitation care.

Ultrasonic cardiogram detection was used to further evaluate the effect of H_2 on the cardiac function of rats after ROSC. As shown in Fig. 1E, cardiac function was evaluated by echocardiography at 4 and 72 h post-ROSC. Echocardiograms were analyzed by the LV trace of M mode images using VevoStrain software. Compared with the Sham group, the LVFS and LVEF were significantly decreased within 4 h following ROSC. However, the LVFS and LVEF significantly increased after ROSC in the CPR + H_2 group (Fig. 1F and G). However, there was no significant difference in levels of LVFS and LVEF between CPR and CPR + H_2 groups at 72 h. Moreover, compared with inhalation normoxia, H_2 therapy also markedly decreased the levels of myocardial injury biomarker CKMB and cTnT in serum after CPR at 4 and 72 h (Fig. 1H and I). Thus, inhalation of H_2 after ROSC significantly improved the cardiac function of rats.

Inhalation of H_2 gas after ROSC improves mitochondrial mass and decreases the number of autophagosomes in rat cardiomyocytes. To investigate the potentially cardioprotective mechanism of the inhalation of H_2 after ROSC, the cross-section and TEM images of LV cardiomyocytes were observed. As shown in Fig. 2A and B, TEM analysis revealed the presence of extensive mitochondrial abnormalities, such as swelling, disorganization and loss of cristae, and the relative mitochondrial mass were significantly deceased in post-resuscitation rat LV cardiomyocytes. However, inhalation of H_2 gas after ROSC significantly decreased the number of abnormal mitochondria and increased the relative mitochondrial mass in rat LVs, and cardiac tissue seemed to have returned to its original morphology at 72 h.

Moreover, autophagic lysosomal structures were common in post-resuscitation rat LV cardiomyocytes, suggesting the activation of autophagic cell death mechanisms. In the CPR groups, a significant decrease in autophagic vesicles was observed at 4 and 72 h in post-resuscitation rats after inhalation of H_2 gas compared with normoxia (Fig. 2A and C).

Inhalation of H_2 gas after ROSC decreases the expression levels of Beclin-1 and suppresses autophagy activation in rat cardiomyocytes. The study next investigated how H_2 affects autophagy in the heart. As show in Fig. 2D-G, western blot analysis revealed increased expression levels of the autophagy promotor protein Beclin1 in normoxic post-resuscitation rat hearts. The expression levels of LC3B were also higher in the CPR + Normoxia groups at 4 and 72 h compared with that in the Sham-Normoxia group, and the ratio of LC3BII/I was also significantly higher, indicating an enrichment of LC3BII. However, the expression levels of p62 were significantly lower in the same groups. There results suggested excessive autophagy activation. However, compared with the CPR + Normoxia groups, H_2 treatment suppressed autophagy activation with significantly lower Beclin-1 and LC3B levels, and a higher p62 protein level. Furthermore, immunohistochemical staining revealed that LC3B levels were significantly higher in cardiomyocytes from rats after ROSC, while H_2 therapy significantly decreased the LC3B protein levels (Fig. 2H and I).

H_2 treatment suppresses H/R-induced autophagy activation in H9C2 cells. All H/R-induced injury experiments were performed on the rat heart embryonic H9C2 cell line. The present study data (Figs. 1 and 2) had shown that H_2-treatment protected cardiomyocytes from CA/resuscitation by inhibiting autophagy activation. To clarify the role of H_2 therapy in CPR-induced myocardial I/R injury, H9C2 cells were subjected to 24 h of hypoxia followed by 4 or 12 h of reoxygenation. According to a previous study protocol, H_2-rich culture medium was used as H_2 treatment for cells *in vitro* (28).

The expression levels of autophagic markers Beclin-1, LC3B and p62 were measured by western blot analysis in H/R-treated H9C2 cells. After H/R, H9C2 cells showed an increase in expression levels of autophagic proteins Beclin-1, LC3B and p62, compared with the control (Fig. 3A and B). H_2 significantly decreased Beclin-1 and LC3B expression in the H/R-treated cardiomyocytes, suggesting the inhibition of autophagy. However, the p62 expression was increased significantly in these H/R + H_2 groups.

Consistent with the western blot analysis, the immunofluorescence staining also indicated that the expression of Beclin-1 and LC3B was increased in H/R-treated cells, while H_2 administration significantly decreased the expression of

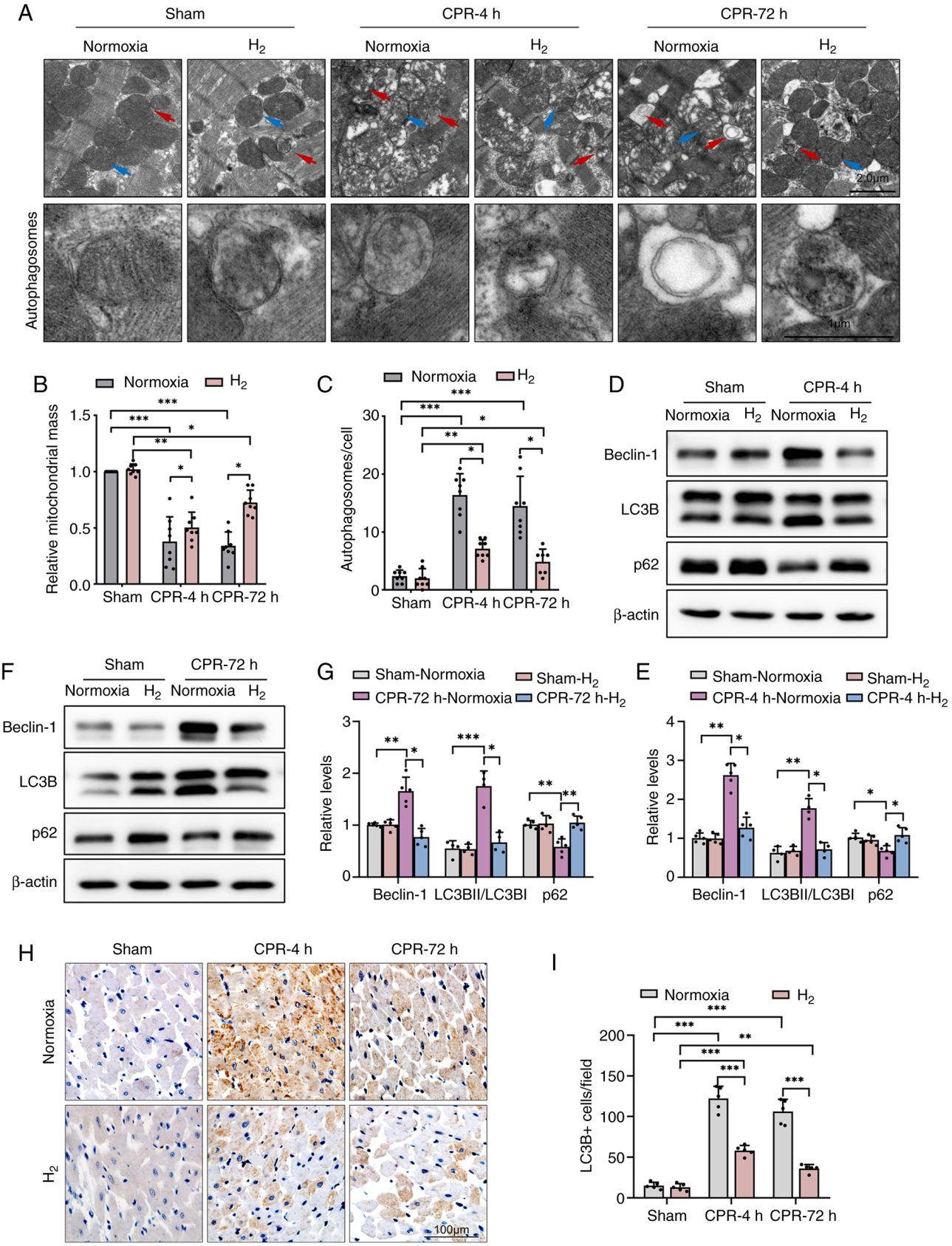

Figure 2. Inhalation of H_2 gas after ROSC improves mitochondrial mass and suppresses autophagy activation in rat cardiomyocytes. (A) The representative images of TEM exhibited the morphology of mitochondria (blue arrows) and autophagosomes (red arrows) in rat cardiomyocytes. The numbers of autophagosomes from at least 10 images in each group were analyzed for the quantification results. Scale bar: 2 μm (top) and 1 μm (bottom). (B) Quantification of mitochondrial mass in TEM images from rat cardiomyocytes (n=8). (C) Quantification of autophagosomes in TEM images from rat cardiomyocytes (n=8). (D-G) The representative images and quantification of immunoblotting analysis of Beclin-1, LC3B and p62 in rat left ventricles after ROSC at 4 and 72 h. (H and I) The representative images and quantification analysis of immunohistochemical staining of LC3B in rat cardiomyocytes (n=5). *P<0.05, **P<0.01 and ***P<0.001. ROSC, return of spontaneous circulation; H2, hydrogen molecule; CPR, cardiopulmonary resuscitation; TEM, transmission electron microscopy; LC3B, microtubule-associated protein 1 light chain 3-B.

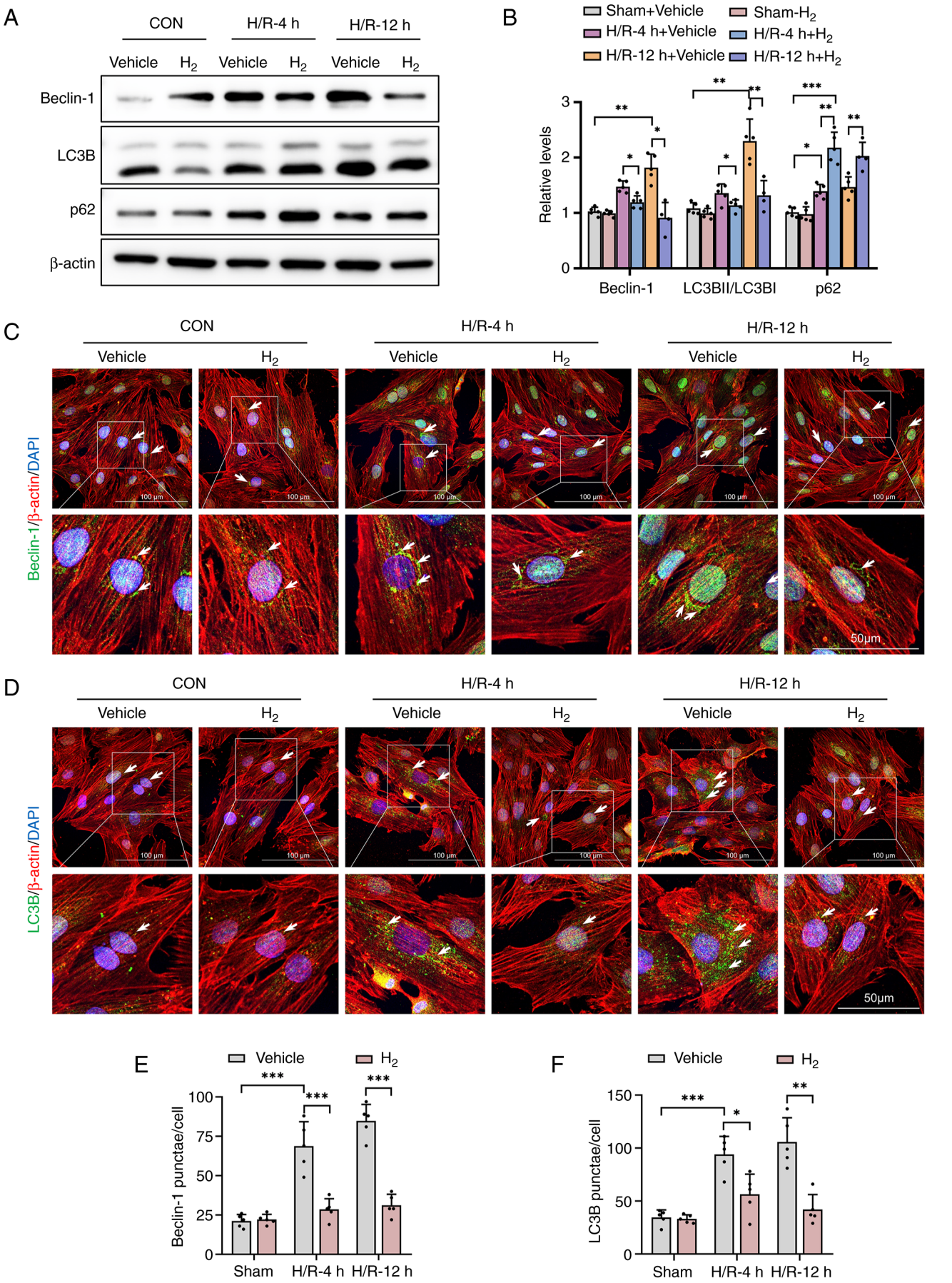

Figure 3. H_2 treatment suppresses H/R-induced autophagy activation in H9C2 cells. (A and B) The representative images and quantification of immunoblotting analysis of Beclin-1, LC3B and p62 in H9C2 cells after H/R. (C-F) The representative images and quantification analysis of immunofluorescence staining of Beclin-1 and LC3B in H9C2 cells (n=5). *P<0.05, **P<0.01 and ***P<0.001. CON, control; H2, hydrogen molecule; H/R, hypoxia/reoxygenation; LC3B, microtubule-associated protein 1 light chain 3-B.

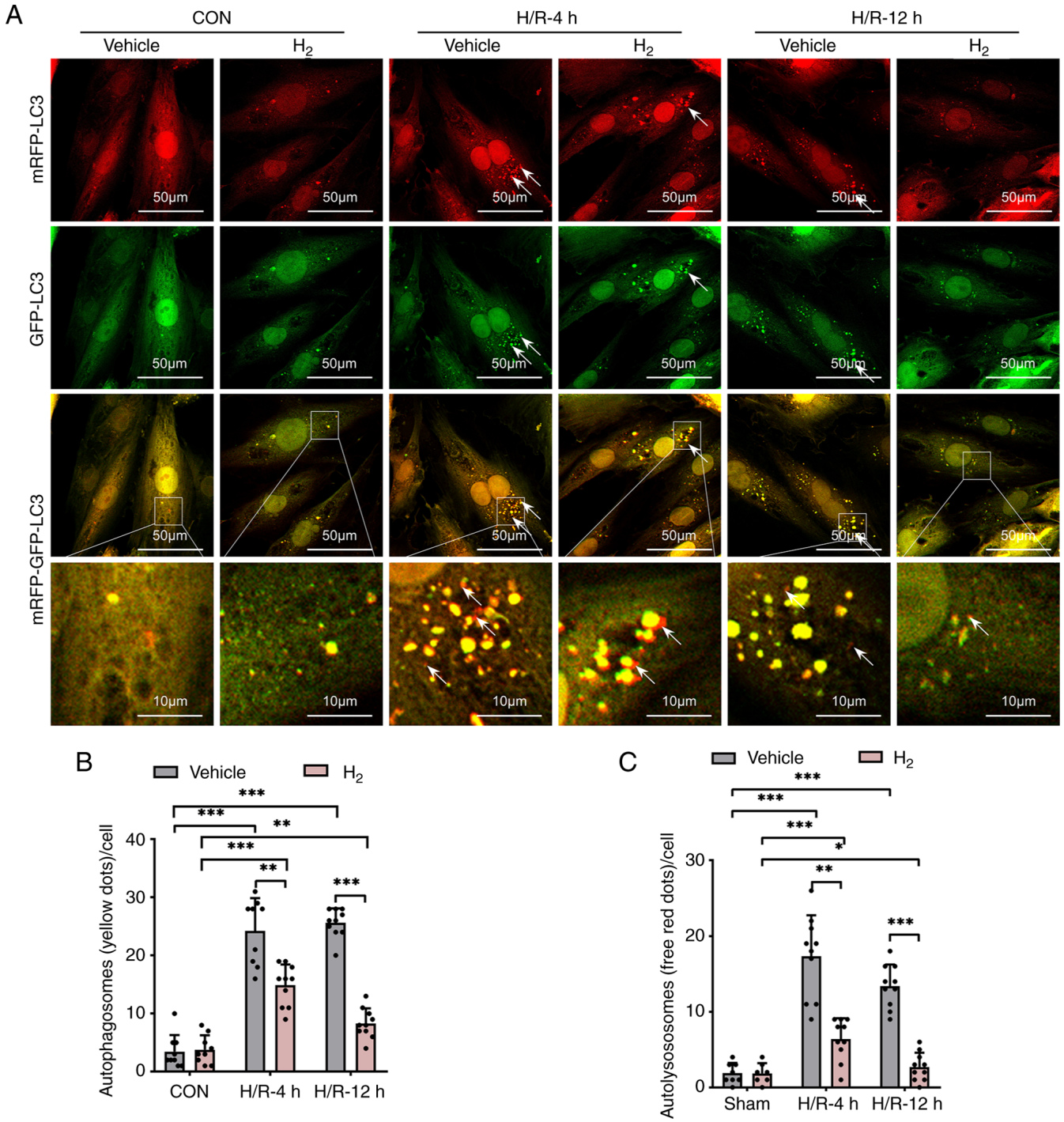

Figure 4. H_2 treatment suppresses H/R-induced accumulation of autophagosomes and autolysosomes in H9C2 cells. (A) The representative images and quantification analysis of the formation of (B) autophagosomes and (C) autolysosomes in H9C2 cells transfected with adenovirus-RFP-GFP-LC3 (n=7-10). Scale bars, 50 μm (top three rows) and 10 μm (bottom row). *P<0.05, **P<0.01 and ***P<0.001. CON, control; H_2, hydrogen molecule; GFP, green fluorescent protein; mRFP, monomeric red fluorescent protein; LC3, microtubule-associated protein 1 light chain 3; H/R, hypoxia/reoxygenation.

these proteins (Fig. 3C-F). These data support the proposal that H_2 protects against H/R-induced injury by decreasing H/R-mediated autophagy.

H_2 treatment suppresses H/R-induced accumulation of autophagosomes and autolysosomes in H9C2 cells. In order to study the formation and process of autophagy, H9C2 cells were transfected with Ad-monomeric RFP (mRFP)-GFP-LC3 and observed at different time points after H/R. As shown in Fig. 4, the generation of both GFP- and mRFP-positive autophagosomes was significantly increased in the H9C2 cells after H/R, while H_2 treatment resulted in a significant decrease in both autophagosome types.

Discussion

The present study investigated the cardioprotective effect of H_2 inhalation after ROSC in a rat CPR model. The results

revealed that H_2 treatment ameliorated animal survival and myocardial abnormalities. The echocardiography at 4 and 72 h after ROSC revealed improved cardiac function in H_2-treated animals compared with the CPR group. Consistent with previous studies (30-33), using electron microscopy analysis, extensive mitochondrial abnormalities and autophagosomes were observed in myocardial cells at 4 and 72 h after ROSC in rats subjected to asphyxial CA/CPR. However, H_2 treatment after ROSC improved mitochondrial morphology and decreased the numbers of autophagosomes. These data demonstrated that the excessive activation of autophagy might exist for a long period in rats subjected to asphyxial CA/CPR. H_2 treatment significantly suppressed autophagy activation.

The present data have defined the role of autophagy in myocardial survival/death after ROSC in an asphyxial CA/CPR model. Furthermore, the role of H_2 in the regulation of autophagy against myocardial injury has not been investigated in asphyxial CA/CPR. In previous studies, autophagy activation was considered as a double-edged sword with both pro-survival and death-causing potential in myocardial I/R injury (34,35). Excessive activation of autophagy leads to degeneration of organelles and drives cell death after reperfusion. Additionally, excess autophagosome clearance has been determined as a major cause of cardiomyocyte death as a result of the observation of autophagosome generation in necrotic cardiomyocytes (36).

In the present study, the data showed that autophagosomes significantly accumulated in cardiomyocytes after ROSC, indicating excessive activation of autophagy. Moreover, the expression levels of Beclin-1 and LC3B were also increased in the LV from 4 to 72 h after asphyxial CA/CPR. Beclin-1, a component of phosphatidylinositol type III kinase complex, has been confirmed to serve a crucial role in regulating autophagosome formation (34). Previous studies have reported the association between Beclin-1 and autophagy-associated cell death in cerebral ischemia (37-40). The present data also revealed that H_2 treatment significantly inhibited autophagy, with decreased Beclin-1 and LC3B expression in cardiomyocytes. Moreover, compared with those in the CPR or H/R groups, the expression levels of p62 significantly decreased in the H_2 treatment groups *in vitro* and *in vivo*, indicating the inhibition of autophagy. However, in contrast to the results in the animal experiments, the expression levels of p62 were significantly increased in the H/R groups in cells. These data may be related to the different amounts of time suffering hypoxia *in vitro* and *in vivo*. In H/R-induced injury experiments, a longer period of hypoxia increased the expression levels of p62 in the H9C2 cells. In summary, these results evaluated the potential cardioprotection of H_2 treatment in CA/CPR.

In vitro, Ad-mRFP-GFP-LC3 were used to observe the formation and process of autophagy. After transfection with Ad-mRFP-GFP-LC3, H9C2 cells ubiquitously express the autophagosome-building microtubule-associated protein LC3 linked with both mRFP and GFP. With autophagy activation, fluorescent signals of mRFP and GFP significantly increase with the formation of phagosomes. Moreover, GFP signals are quenched where autophagosomes eventually fuse with lysosomes (41). In the *in vitro* H/R experiments of the present study, a decrease in autophagy-associated proteins (Beclin-1 and LC3B) and autophagosomes was observed after H_2 treatment, which suggested that the cell homeostasis mechanisms of H_2 therapy in cardioprotection are associated with the inhibition of autophagy. In previous studies, the anti-apoptotic properties of H_2 have also been demonstrated, with the alleviation of hyperoxia inducing lung epithelial cell apoptosis via the induction of Bcl-2 and the suppression of Bax expression (42-44). These results revealed a potential mechanism of H_2-mediated cell fate under stress.

In conclusion, the present study demonstrated that H_2 inhalation after resuscitation suppressed autophagy activation and improved cardiac function and survival in a rat model of CA. These findings suggest a potentially novel and easily applicable treatment for cardiac dysfunction in post-cardiac arrest syndrome; however, further investigation is required to confirm the cell homeostasis mechanisms of H_2 therapy for cardioprotection.

Acknowledgements

Not applicable.

Funding

This study was supported by the State Key Program of the National Natural Science Foundation of China (grant no. 82030059), the National Natural Science Foundation of China (grant nos. 81772036, 82072144, 81671952, 81873950 and 81873953), the National Key R&D Program of China (grant nos. 2020YFC1512700, 2020YFC1512705, 2020YFC1512703 and 2020YFC0846600), the National S&T Fundamental Resources Investigation Project (grant no. 2018FY100600 and 2018FY100602), the Taishan Pandeng Scholar Program of Shandong Province (grant no. tspd20181220), the Taishan Young Scholar Program of Shandong Province (grant nos. tsqn20161065 and tsqn201812129), the Youth Top-Talent Project of National Ten Thousand Talents Plan, Qilu Young Scholar Program and the Fundamental Research Funds of Shandong University (grant no. 2018JC011) and the Inner Mongolia Department of Education (grant no. NJZY22143).

Availability of data and materials

The datasets used and/or analyzed during the current study are available from the corresponding author on reasonable request.

Authors' contributions

XG, TX, XH and YC conceived and designed the study. XG, XF, XY, TX, JL, JG and XZ performed the study. XG, TX, SW, QY, JW and XF contributed to the data analysis. XG, TX, XH and YC wrote the manuscript. XG and TX confirm the authenticity of all the raw data. All authors have read and approved the manuscript.

Ethics approval and consent to participate

All animal experiments were approved by the Animal Care and Use Committee of the Qilu Hospital of Shandong University (Jinan, China; approval no. KYLL-2020-ZM-122), and adhered to the guidelines from the Care and Use of Laboratory Animals.

Patient consent for publication

Not applicable.

Competing interests

The authors declare that they have no competing interests.

References

1. Brady WJ, Mattu A and Slovis CM: Lay Responder care for the adult victim of out-of-hospital cardiac arrest. Reply. N Engl J Med 382: e24, 2020.
2. Dankiewicz J, Cronberg T, Lilja G, Jakobsen JC, Levin H, Ullén S, Rylander C, Wise MP, Oddo M, Cariou A, *et al*: Hypothermia versus normothermia after out-of-hospital cardiac arrest. N Engl J Med 384: 2283-2294, 2021.
3. Couzin-Frankel J: Clinical trials test potential CPR upgrade. Science 363: 913-914, 2019.
4. He M, Gong Y, Li Y, Mauri T, Fumagalli F, Bozzola M, Cesana G, Latini R, Pesenti A and Ristagno G: Combining multiple ECG features does not improve prediction of defibrillation outcome compared to single features in a large population of out-of-hospital cardiac arrests. Crit Care 19: 425, 2015.
5. Shao F, Li CS, Liang LR, Li D and Ma SK: Outcome of out-of-hospital cardiac arrests in Beijing, China. Resuscitation 85: 1411-1417, 2014.
6. Bray JE, Bernard S, Cantwell K, Stephenson M and Smith K; VACAR Steering Committee: The association between systolic blood pressure on arrival at hospital and outcome in adults surviving from out-of-hospital cardiac arrests of presumed cardiac aetiology. Resuscitation 85: 509-515, 2014.
7. Chenoune M, Lidouren F, Adam C, Pons S, Darbera L, Bruneval P, Ghaleb B, Zini R, Dubois-Randé JL, Carli P, *et al*: Ultrafast and whole-body cooling with total liquid ventilation induces favorable neurological and cardiac outcomes after cardiac arrest in rabbits. Circulation 124: 901-911, 1-7, 2011.
8. Xu H, Li Y, Liu R, Wu L, Zhang C, Ding N, Ma A, Zhang J and Xie X: Protective effects of ghrelin on brain mitochondria after cardiac arrest and resuscitation. Neuropeptides 76: 101936, 2019.
9. Nguyen Thi PA, Chen MH, Li N, Zhuo XJ and Xie L: PD98059 protects brain against cells death resulting from ROS/ERK activation in a cardiac arrest rat model. Oxid Med Cell Longev 2016: 3723762, 2016.
10. Penna C, Perrelli MG and Pagliaro P: Mitochondrial pathways, permeability transition pore, and redox signaling in cardioprotection: Therapeutic implications. Antioxid Redox Signal 18: 556-599, 2013.
11. Cui R, Liu S, Wang C, Liu T, Ren J, Jia Y, Tong Y, Liu C and Zhang J: Methane-rich saline alleviates CA/CPR brain injury by inhibiting oxidative stress, microglial activation-induced inflammatory responses, and ER stress-mediated apoptosis. Oxid Med Cell Longev 2020: 8829328, 2020.
12. Zhang R, Liu B, Fan X, Wang W, Xu T, Wei S, Zheng W, Yuan Q, Gao L, Yin X, *et al*: Aldehyde dehydrogenase 2 protects against post-cardiac arrest myocardial dysfunction through a novel mechanism of suppressing mitochondrial reactive oxygen species production. Front Pharmacol 11: 373, 2020.
13. Lellouche F and L'Her E: Usual and advanced monitoring in patients receiving oxygen therapy. Respir Care 65: 1591-1600, 2020.
14. Soar J, Böttiger BW, Carli P, Couper K, Deakin CD, Djärv T, Lott C, Olasveengen T, Paal P, Pellis T, *et al*: European resuscitation council guidelines 2021: Adult advanced life support. Resuscitation 161: 115-151, 2021.
15. Chu DK, Kim LH, Young PJ, Zamiri N, Almenawer SA, Jaeschke R, Szczeklik W, Schünemann HJ, Neary JD and Alhazzani W: Mortality and morbidity in acutely ill adults treated with liberal versus conservative oxygen therapy (IOTA): A systematic review and meta-analysis. Lancet 391: 1693-1705, 2018.
16. Allardet-Servent J, Sicard G, Metz V and Chiche L: Benefits and risks of oxygen therapy during acute medical illness: Just a matter of dose! Rev Med Interne 40: 670-676, 2019.
17. Vereczki V, Martin E, Rosenthal RE, Hof PR, Hoffman GE and Fiskum G: Normoxic resuscitation after cardiac arrest protects against hippocampal oxidative stress, metabolic dysfunction, and neuronal death. J Cereb Blood Flow Metab 26: 821-835, 2006.
18. Zhou G, Goshi E and He Q: Micro/nanomaterials-augmented hydrogen therapy. Adv Healthc Mater 8: e1900463, 2019.
19. Buret AG, Allain T, Motta JP and Wallace JL: Effects of hydrogen sulfide on the microbiome: From toxicity to therapy. Antioxid Redox Signal 36: 211-219, 2022.
20. Hardeland R: Hydrogen therapy: A future option in critical care? Crit Care Med 40: 1382-1383, 2012.
21. Ohsawa I, Ishikawa M, Takahashi K, Watanabe M, Nishimaki K, Yamagata K, Katsura K, Katayama Y, Asoh S and Ohta S: Hydrogen acts as a therapeutic antioxidant by selectively reducing cytotoxic oxygen radicals. Nat Med 13: 688-694, 2007.
22. Liu CL, Zhang K and Chen G: Hydrogen therapy: From mechanism to cerebral diseases. Med Gas Res 6: 48-54, 2016.
23. Durante W: Hydrogen sulfide therapy in diabetes-accelerated atherosclerosis: A whiff of success. Diabetes 65: 2832-2834, 2016.
24. Zhang L, Yu H, Tu Q, He Q and Huang N: New approaches for hydrogen therapy of various diseases. Curr Pharm Des 27: 636-649, 2021.
25. Sano M, Suzuki M, Homma K, Hayashida K, Tamura T, Matsuoka T, Katsumata Y, Onuki S and Sasaki J: Promising novel therapy with hydrogen gas for emergency and critical care medicine. Acute Med Surg 5: 113-118, 2017.
26. Hayashida K, Sano M, Kamimura N, Yokota T, Suzuki M, Ohta S, Fukuda K and Hori S: Response to letter regarding article, 'hydrogen inhalation during normoxic resuscitation improves neurological outcome in a rat model of cardiac arrest independently of targeted temperature management'. Circulation 132: e148, 2015.
27. Hayashida K, Sano M, Kamimura N, Yokota T, Suzuki M, Ohta S, Fukuda K and Hori S: Hydrogen inhalation during normoxic resuscitation improves neurological outcome in a rat model of cardiac arrest independently of targeted temperature management. Circulation 130: 2173-2180, 2014.
28. Chen H, Xie K, Han H, Li Y, Liu L, Yang T and Yu Y: Molecular hydrogen protects mice against polymicrobial sepsis by ameliorating endothelial dysfunction via an Nrf2/HO-1 signaling pathway. Int Immunopharmacol 28: 643-654, 2015.
29. Zhou Z, Vidales J, González-Reyes JA, Shibata B, Baar K, Rutkowsky JM and Ramsey JJ: A 1-month ketogenic diet increased mitochondrial mass in red gastrocnemius muscle, but not in the brain or liver of middle-aged mice. Nutrients 13: 2533, 2021.
30. Lu Y, Zeng X, Jing X, Yin M, Chang MMP, Wei H, Yang Y, Liao X, Dai G and Hu C: Pre-arrest hypothermia improved cardiac function of rats by ameliorating the myocardial mitochondrial injury after cardiac arrest. Exp Biol Med (Maywood) 244: 1186-1192, 2019.
31. Ji X, Bradley JL, Zheng G, Ge W, Xu J, Hu J, He F, Shabnam R, Peberdy MA, Ornato JP, *et al*: Cerebral and myocardial mitochondrial injury differ in a rat model of cardiac arrest and cardiopulmonary resuscitation. Biomed Pharmacother 140: 111743, 2021.
32. Huang Y, Gao X, Zhou X, Xie B, Zhang Y, Zhu J and Zhu S: Mitophagy in the hippocampus is excessive activated after cardiac arrest and cardiopulmonary resuscitation. Neurochem Res 45: 322-330, 2020.
33. Cao S, Sun Y, Wang W, Wang B, Zhang Q, Pan C, Yuan Q, Xu F, Wei S and Chen Y: Poly (ADP-ribose) polymerase inhibition protects against myocardial ischaemia/reperfusion injury via suppressing mitophagy. J Cell Mol Med 23: 6897-6906, 2019.
34. Shi B, Ma M, Zheng Y, Pan Y and Lin X: mTOR and beclin1: Two key autophagy-related molecules and their roles in myocardial ischemia/reperfusion injury. J Cell Physiol 234: 12562-12568, 2019.
35. Wu MY, Yiang GT, Liao WT, Tsai AP, Cheng YL, Cheng PW, Li CY and Li CJ: Current mechanistic concepts in ischemia and reperfusion injury. Cell Physiol Biochem 46: 1650-1667, 2018.
36. Kroemer G and Levine B: Autophagic cell death: The story of a misnomer. Nat Rev Mol Cell Biol 9: 1004-1010, 2008.
37. Rami A, Langhagen A and Steiger S: Focal cerebral ischemia induces upregulation of beclin 1 and autophagy-like cell death. Neurobiol Dis 29: 132-141, 2008.
38. Grishchuk Y, Ginet V, Truttmann AC, Clarke PG and Puyal J: Beclin 1-independent autophagy contributes to apoptosis in cortical neurons. Autophagy 7: 1115-1131, 2011.

39. Guo D, Ma J, Yan L, Li T, Li Z, Han X and Shui S: Down-regulation of lncrna MALAT1 attenuates neuronal cell death through suppressing beclin1-dependent autophagy by regulating Mir-30a in cerebral ischemic stroke. Cell Physiol Biochem 43: 182-194, 2017.
40. Xu T, Guo J, Wei M, Wang J, Yang K, Pan C, Pang J, Xue L, Yuan Q, Xue M, *et al*: Aldehyde dehydrogenase 2 protects against acute kidney injury by regulating autophagy via the Beclin-1 pathway. JCI Insight 6: e138183, 2021.
41. Kaizuka T, Morishita H, Hama Y, Tsukamoto S, Matsui T, Toyota Y, Kodama A, Ishihara T, Mizushima T and Mizushima N: An autophagic flux probe that releases an internal control. Mol Cell 64: 835-849, 2016.
42. Kawamura T, Wakabayashi N, Shigemura N, Huang CS, Masutani K, Tanaka Y, Noda K, Peng X, Takahashi T, Billiar TR, *et al*: Hydrogen gas reduces hyperoxic lung injury via the Nrf2 pathway in vivo. Am J Physiol Lung Cell Mol Physiol 304: L646-L656, 2013.
43. Ge L, Yang M, Yang NN, Yin XX and Song WG: Molecular hydrogen: A preventive and therapeutic medical gas for various diseases. Oncotarget 8: 102653-102673, 2017.
44. Ohta S: Molecular hydrogen as a preventive and therapeutic medical gas: Initiation, development and potential of hydrogen medicine. Pharmacol Ther 144: 1-11, 2014.